Zoology 157 (2023) 126079

Contents lists available at ScienceDirect

Zoology

journal homepage: www.elsevier.com/locate/zool

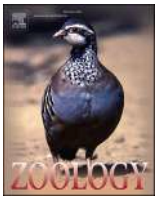

Morphological and physiological traits of the respiratory system in *Iguana iguana* and other non-avian reptiles

André Luis da Cruz [a,*], Bruno Vilela [a], Wilfried Klein [b]

[a] *Institute of Biology, Federal University of Bahia, Rua Barão de Jeremoabo 147, Ondina, CEP 40170–115 Salvador, Bahia, Brazil*
[b] *School of Philosophy, Sciences and Literature of Ribeirão Preto, University of São Paulo, Avenida Bandeirantes 3900. Monte Alegre, CEP 14040–900 Ribeirão Preto, São Paulo, Brazil*

ARTICLE INFO

Keywords:
Gas exchanger
Stereology
Oxygen transport cascade
Dimensionality reduction
Evolutionary approach

ABSTRACT

Functional morphology considers form and function to be intrinsically related. To understand organismal functions, a detailed knowledge of morphological and physiological traits is necessary. Regarding the respiratory system, the combined knowledge about pulmonary morphology and respiratory physiology is fundamental to understand how animals exchange gases and regulate critical functions to sustain metabolic activity. In the present study, the paucicameral lungs of *Iguana iguana* were analyzed morphometrically through stereological analysis using light and transmission electron images and compared with unicameral and multicameral lungs of six other non-avian reptiles. The morphological data were combined with physiological information to perform a principal component analysis (PCA) and phylogenetic tests of the relationship of the respiratory system. *Iguana iguana*, *Lacerta viridis*, and *Salvator merianae* presented similar pulmonary morphologies and physiologies when compared to *Varanus examthematicus*, *Gekko gecko*, *Trachemys scripta,* and *Crocodylus niloticus*. The former species showed an elevated respiratory surface area ($\%A_R$), a high diffusion capacity, a low volume of total parenchyma (V_P), a low percentage of parenchyma concerning the lung volume (V_L), and a higher surface/volume ratio of the parenchyma (S_{AR}/V_P), with high respiratory frequency (f_R) and consequently total ventilation. The total parenchymal surface area (S_A), effective parenchymal surface-to-volume ratio (S_{AR}/V_P), respiratory surface area (S_{AR}), and anatomical diffusion factor (ADF) showed a phylogenetic signal, evidence that the morphological traits are more strongly correlated with the species' phylogeny than the physiological traits. In sum, our results indicated that the pulmonary morphology is intrinsically related to physiological traits of the respiratory system. Furthermore, phylogenetic signal tests also indicate that morphological traits are more likely to be evolutionary conserved than physiological traits, suggesting that evolutive physiological adaptations in the respiratory system could happen faster than morphological changes.

1. Introduction

Amniotes present vast morphological variation in lung structure, especially concerning the degree of pulmonary subdivision and type, and distribution of gas exchange epithelium (Perry and Sander, 2004). Observations of the pulmonary embryological development in Madagascar ground geckos provide evidence that the last common ancestor of amniotes possessed complex multichambered lungs that gave rise to the bronchioalveolar mammalian lung as well as the multicameral lungs of archosaurs and testudines (Lambertz et al., 2015; Perry et al., 2019). In this scenario, the widespread unicameral lung type of many lepidosaurs would be a plesiomorphic character maintained from ancestral lepidosaurs who underwent miniaturization and concomitantly lost the multichambered lung — whereas the more divided paucicameral and multicameral lungs (present in Iguania, Gekkota, Varanoidea; see Perry, 1998 for details) would represent secondary modifications (Lambertz et al., 2015).

Perry et al. (2019) commented that if the evolution of the pulmonary structure could be seen separately from all other organ systems, and if someone could establish an absolute functional criterion for that evolution, an ideal lung would possess two different sets of properties: one for the pump, and another for the gas exchanger. The pump should move large quantities of air while having substantial compliance needing a minimum amount of work to perform lung ventilation.

* Corresponding author.
E-mail addresses: cruz.andre@ufba.br (A.L. da Cruz), bruno.vilela@ufba.br (B. Vilela), wklein@usp.br (W. Klein).

https://doi.org/10.1016/j.zool.2023.126079
Received 30 March 2022; Received in revised form 8 February 2023; Accepted 18 February 2023
Available online 22 February 2023

On the other hand, the ideal gas exchanger should possess a large surface area, good air convection of respiratory surfaces, maximum exposure of capillary surfaces, and an effective diffusion capacity per unit of pulmonary surface area (Perry, 1983). When the oxygen diffusion capacity is determined morphometrically, the values are always greater than the ones measured physiologically. This can be explained by the fact that morphometric data are not influenced by physiological limitations related to the transport of oxygen towards the lungs and through respiratory epithelium into the blood. In this oxygen transport cascade, ventilation-perfusion, diffusion-perfusion inhomogeneities, pulmonary shunting, or blood oxygen-carrying capacities may reduce the amount of oxygen absorbed at the air/blood interface (Wang et al., 1998; Wang and Hicks, 2002).

Among Squamata, the various aspects of the oxygen transport cascade have only been extensively studied in a few species, such as *Crotalus durissus*, *Salvator merianae*, and *Iguana iguana*. Due to its widespread distribution, ease of reproduction in captivity, and relatively large size, the green iguana (*Iguana iguana*) has been widely used as an experimental model to understand different aspects of the gas transport cascade, such as lung ventilation (Giordano and Jackson, 1973; Carrier, 1987; Brainerd et al., 2016), circulation (Tucker, 1968; Wood and Moberly, 1970; Baker and White, 1970; Baker et al., 1972; Gleeson et al., 1980; Mitchell et al., 1981; Farmer and Hicks, 2000; Wang et al., 1997), or oxygen consumption (Maxwell et al., 2003; Sartori et al., 2017).

The paucicameral (transitional) lungs of *Iguana iguana* each consist of two chambers separated by a longitudinal septum. The cranio-medial chamber is composed of faveolar parenchyma while the caudal chamber exhibits faveolar parenchyma in its cranial portion but trabecular parenchyma in the caudal part, resulting in a heterogeneously distributed respiratory epithelium. The uneven parenchymal distribution in the two chambers is associated with greater specialization of the cranial chamber for gas exchange. In contrast, the caudal chamber seems better equipped to perform a more ventilatory function, moving air in and out of the lungs (Peixoto et al., 2018). There is evidence that airflow from the lungs of *I. iguana* is unidirectional (Cieri et al., 2014).

However, this view was disputed by Perry et al. (2019), arguing that within a single-chambered lung, any centralized jet stream of inspired air would show unidirectional lateral backflow once it hits the caudal end of the lung.

This study investigated whether *Iguana iguana* lung characteristics indicate morphofunctional and physiological differences compared to other non-avian reptiles, following our previous study of iguana lung morphometrics (Peixoto et al., 2018). Therefore, we determined stereological parameters of *I. iguana* lungs to analyze their functionality and compared them with morphometric data from other reptilian lungs. Only few species had detailed morphological and physiological data available in the literature that could be included into our analysis, this included the lizards *Varanus exanthematicus*, *Lacerta viridis*, *Salvator merianae*, *Gekko gecko*, the crocodilian *Crocodylus niloticus*, and the chelonian *Trachemys scripta*. Subsequently, we investigated relationships between morphometric data of the reptilian respiratory system and physiological variables to integrate morphology and physiology to understand the stages of pulmonary gas exchange in *I. iguana*. Furthermore, we verified whether morphological and physiological traits are phylogenetically related, thereby showing whether form and function are evolutionarily linked.

2. Material and methods

2.1. Animals

The same *Iguana iguana* individuals use by Peixoto et al. (2018) provided the tissue samples analyzed in the present study. Briefly, animals of different body masses (M_B: 0.020, 0.026, 0.319, 0.546, and 2.4 kg) were obtained from the same population of animals held and reproduced at the Jacarezário, São Paulo State University "Julio de Mesquita Filho" Rio Claro, SP, Brazil. The animals were euthanized by an overdose of Sodium Thiopental (100 $mg.kg^{-1}$), administered intraperitoneally (018/2014 Protocol of the Committee on Animal Use and Ethics, IBIO/UFBA). Subsequently, the lungs were fixed using intratracheal instillation of glutaraldehyde 5% in 0.2 M phosphate buffer (pH 7.4, 380 mOsm) at a pressure of 20 cmH_2O for 12 h. Following fixation, the lungs were removed and stored for up to 10 days in glutaraldehyde 0.5% stock solution in 0.2 M phosphate buffer (pH 7.4; 380 mOsm) for light and electron microscopical processing.

2.2. Histological processing

The determination of the total lung volume of the five iguanas followed the results of Peixoto et al. (2018). The total lung volume was determined by the Cavalieri method, which estimates the total volume and area of cross sections multiplied by the distance between the sections (Cruz-Orive & Weibel, 1990). For this purpose, the size of each lung was measured in a craniocaudal direction, and ten cross sections were performed from a random starting point and at fixed distances, based on the total length of each lung. A test system was superimposed onto the cross sections, and the number of points covering lung parenchymal and lung lumen were counted. The total volume (V_L) of the lungs was given by: $V = T.a/p.\Sigma Pi$, where "T" is the distance between sequential sections, "a/p" is the area represented by each point, and "Pi" is the number of points over the parenchyma and lumen. The same methodology was applied to estimate the parenchymal and lumen volume separately by counting the points over each structure.

The samples used for the light microscopy were dehydrated in a graded series of ethanol with their pleural surface facing down. They were systematically rotated and sectioned to obtain vertical uniform sections (VUR), according to Howard and Reed (2005). Subsequently, they were embedded in methacrylate (Historesina® Leica). Histological sections of 5 μm were cut using a manual Zeiss Hyrax M15 microtome, mounted on slides, stained with toluidine blue (1%), and photomicrographed (Axiphot II Carl Zeiss, camera Axiocam MrC3 and capture software Axio Vision 4.8).

The samples for transmission electron microscopy were post-fixed in osmium tetroxide (1%), 0.8% potassium ferrocyanide, and 5 mM calcium chloride in 0.1 M sodium cacodylate buffer (pH 7.4) for one hour. They were washed three times for ten minutes each in the same buffer, dehydrated in a graded series of acetone, followed by three successive baths of 100% acetone and subsequent replacement of the acetone and Polybed® resin (1:1) for 6 h. Afterward, the samples were transferred to pure resin, where they remained until polymerization. Semithin (0.5 μm) and ultrathin (80 nm) sections were performed using an ultramicrotome Leica EM UC7. The ultrathin sections were stained using uranyl acetate and lead citrate and analyzed with a transmission electron microscope JEOL 1230.

2.3. Stereological analysis

The surface area per unit volume (surface density = S_V) and the total lung surface (S) were calculated by counting intersections with the lung surface and points on the same tissue using a cycloid arc test system, following Howard and Reed (2005), $S_V = 2.\ \Sigma I_i/(I/p.\Sigma P_i)$ and $S = S_V.\ V$ where P_i is the number of points on the tissue, I/p is the length of the cycloid arc by point of the test system. Ii is the number of the count of intersections with the respiratory surface under light microscopy (Fig. 1A).

The harmonic mean thickness of the air-blood diffusion barrier (τht) was determined for each individual using transmission electron micrographs overlapping a test system of cycloid arcs (Fig. 1B). The length of each line segment of the test system connecting the surfaces of the epithelium with an erythrocyte was measured with a logarithmic ruler, according to the method of Perry (1983). The anatomical diffusion factor (ADF) was calculated as the ratio of the respiratory surface area to

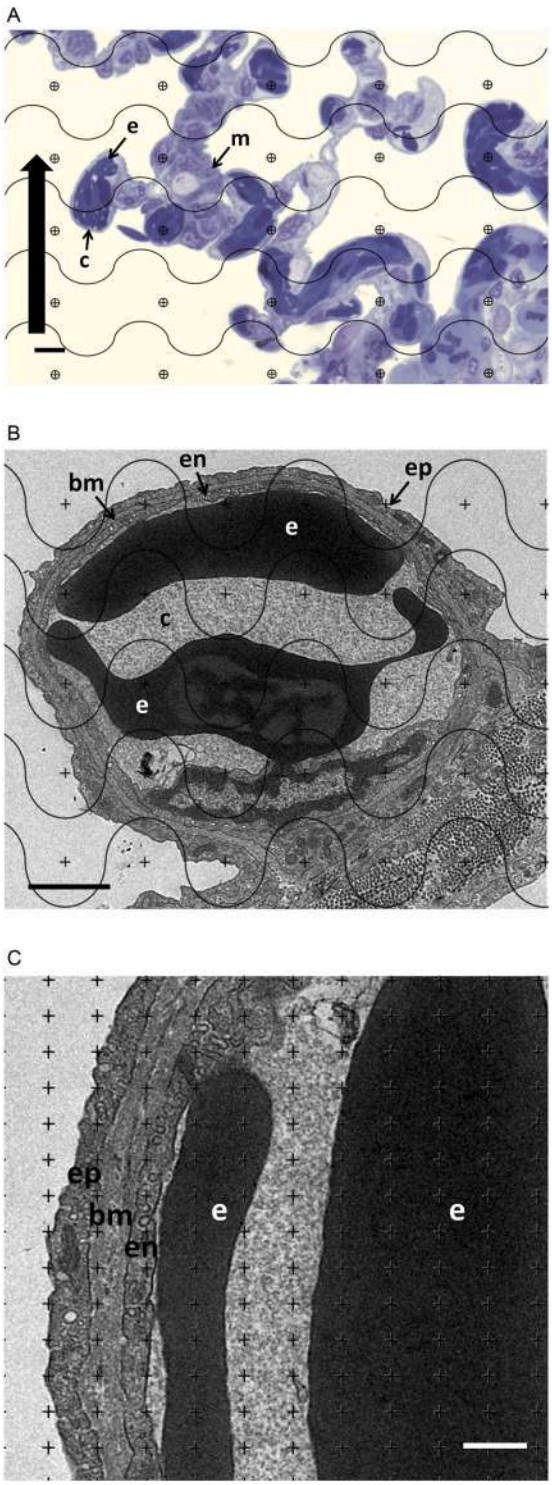

Fig. 1. A) Light micrograph of a vertical section of the parenchymal lung of *Iguana iguana* showing a capillary network with capillaries (c) arranged on both sides supported by non-trabecular smooth muscle (m). The test array was superimposed on the microscopic image to estimate the stereological measurements of lung components. The thick arrow indicates the vertical axis of the lung section and test array. Erythrocytes (e). Scale bar: 10 μm. B) Merz grid superimposed on the transmission electron micrograph of epithelial surface. Intersection points (arrows) indicate starting points for randomly oriented blood–air barrier measurements. Scale bar: 2 μm. C) Square lattice graticule to perform point counting to estimate volume proportion of blood–air barrier components superimposed on a transmission electron micrograph. Epithelium (ep), basal membrane (bm), and endothelium (en). Scale bar: 2 μm.

body mass divided by the harmonic mean thickness of the diffusion barrier (τht) (Moraes et al., 2005; Howard and Reed, 2005).

2.4. Estimation of morphological diffusion capacity for oxygen

Based on the values obtained for ADF, we calculated the morphological diffusing capacity for oxygen (DtO_2) of the iguana lungs as $DtO_2 = KtO_2$. ADF, where KtO_2 represents Krogh's diffusion constant for oxygen in lung tissue. Since KtO_2 has not yet been determined for reptilian lungs, the KtO_2 as determined by Grote (1967) for rat lung tissue was assumed for the parts of the diffusion barrier composed by lung epithelium and capillary endothelium, whereas the KtO_2 for frog connective tissue (Bartels, 1971) was applied to the parts of the diffusion barrier being composed of connective tissue or basal lamina.

This method to calculate morphometric diffusion capacity followed Moraes et al. (2005). We estimated the relative proportions of epithelium/endothelium and connective tissue by point-counting our electron micrograph images (Fig. 1C).

While Grote (1967) measured KtO_2 for rat lung tissue at 20, 30, and 37 °C, the KtO_2 for frog connective tissue is only available for 20 °C. Therefore, we corrected the frog connective tissue KtO_2, assuming a 1% change per °C, following Krogh (1919) to obtain corresponding values for 20 and 30 °C (Table 1).

2.5. Principal components analysis

We obtained the same morphometric variables measured in the present study for other species of non-avian reptiles available in Perry et al. (1994) (Table 2), as well as physiological variables describing respiratory system function in the same species (Table 3). The stereological morphometric data of the lungs of *I. iguana* were compared with those of other non-avian reptiles using a principal component analysis (PCA) based on a correlation matrix. This also allowed us to verify whether morphometric variables obtained using stereological principles correlated with physiological parameters. All quantitative data obtained from Perry et al. (1994) represented the mean values and were normalized per kg M_B to facilitate comparisons. Note, however, that the variations were not provided for all species; hence, the comparisons presented in our results (see Section 3.2) should be interpreted with caution.

2.6. Phylogenetic analysis

We obtained the phylogenetic tree hypothesis including all species from the TimeTree project (Kumar et al. 2022). We calculated the phylogenetic signal for all physiological and morphological traits using Blomberg's k. Values of k closer to 1 indicate that the character follows a distribution expected under a Brownian Motion evolutionary mode. In contrast, values closer to 0 indicate the absence of a phylogenetic signal. Blomberg's k can also show values above 1, meaning that the trait is more evolutionary conserved than expected under a Brownian motion evolutionary mode. The p-values of Blomberg's *k* were generated using

Table 1
Krogh's diffusion constants for epithelium/endothelium ($Kt_{e/e}$) and connective tissue/basal membrane ($Kt_{c/b}$) used to estimate pulmonary oxygen diffusion capacity.

Temperature (°C)	$Kt_{e/e}$[a] (10^{-5} $cm^2.min^{-1}.mmHg^{-1}$)	$Kt_{c/b}$ (10^{-5} $cm^2.min^{-1}.mmHg^{-1}$)
20	2.63[a]	1.51[b]
30	2.96[a]	1.67[c]
37	3.29[a]	1.79[c]

[a] value taken from Grote (1967)
[b] value taken from Bartels (1971)
[c] value calculated from Bartels' (1971) 20 °C value

Table 2
Morphometric comparison of the lungs of *Iguana iguana* with those of other non-avian reptiles. Data from Perry et al. (1994) except for *I. iguana* (this study). Body mass (M_B); total lung volume (V_L); parenchymal volume (%P); parenchymal volume (V_P); total parenchymal surface area (S_A); respiratory surface area (%A_R); effective surface-to-volume ratio in parenchyma (S_{AR}/V_P); respiratory surface area (S_{AR}); harmonic mean thickness (τht); anatomical diffusion factor (ADF). All quantitative data obtained from Perry et al. (1994) represent mean values and were normalized per kg M_B to facilitate comparisons.

	M_B (kg)	V_L (ml. kg^{-1})	%P (% of V_L)	V_P (ml. kg^{-1})	S_A (10^3 cm^2. kg^{-1})	%A_R (% of S_A)	S_{AR}/V_P (cm^2. cm^{-3})	S_{AR} ($10^3 cm^2$. kg^{-1})	τht (μm)	ADF ($10^3.cm^2.\mu m^{-1}.kg^{-1}$)
Iguana iguana	0.66	277.56	17.89	48.02	2.90	52.70	95.31	4.40	0.63	6.95
Varanus exanthematicus	1.00	306.70	28.70	83.20	6.13	88.60	65.30	5.43	0.65	8.35
Lacerta viridis	0.02	94.80	34.60	32.00	6.07	70.00	129.60	4.25	0.53	8.01
Salvator merianae	0.72	84.40	26.00	22.00	3.76	78.20	133.60	2.94	0.46	6.39
Gekko gecko	0.19	164.60	11.70	19.30	1.38	69.30	36.40	0.95	1.08	0.90
Crocodylus niloticus	1.00	113.10	42.00	39.70	1.38	50.00	15.30	0.66	1.40	0.63
Trachemys scripta	0.44	262.30	44.90	117.80	2.49	82.70	18.00	2.06	0.50	4.20

Table 3
Respiratory physiology parameters ($\dot{V}O_2$: oxygen consumption; V_T: tidal volume; $\dot{V}e$: pulmonary ventilation; f_R: breathing frequency) of non-avian reptile species, based on the respective references within a temperature range of 30 – 35 °C, used in PCAs. All quantitative data represent mean values.

	$\dot{V}O_2$ ($ml.min^{-1}.kg^{-1}$)	V_T ($ml.kg^{-1}$)	$\dot{V}e$ ($ml.min^{-1}.kg^{-1}$)	f_R (min^{-1})	Source
Iguana iguana	4.14	15.60	105.40	6.90	Giordano and Jackson, 1973
Varanus exanthematicus	1.20	19.70	25.20	1.40	Hicks et al. 2000
Lacerta viridis	0.28	3.67	157.89	43.06	Cragg, 1978
Salvator merianae	2.70	10.50	37.60	3.60	Klein et al. 2003
Gekko gecko	2.30	10.00	280.00	34.00	Chiu et al. 1986
Crocodylus niloticus	0.55	11.00	29.12	3.45	Brown and Loveridge, 1981
Trachemys scripta	0.88	8.50	9.50	1.20	Jackson, 1971

permutations tests with 100 repetitions implemented in the Phytools package, function "phylosig" (Revell, 2012), for the R software version 4.1.0 (R core Team, 2021).

3. Results

3.1. Lung morphometry of Iguana iguana

The average parenchymal volume corresponded to 17.29% of the total volume of the lungs. In comparison, the average density of the respiratory surface (%A_R) represented 52.70% of the proportion of the respiratory surface of the lung (S_{AR}= 4.40 ± 0.95 $10^3.cm^2.kg^{-1}$) of *Iguana iguana*, resulting in an effective surface-to-volume ratio in parenchyma of 95.31 $cm^2.cm^{-3}$. The harmonic means thickness of the air-blood diffusion barrier (τht) varied between 0.51 and 0.76 μm, and the anatomical diffusion factor (ADF) was calculated as 6.95 ± 1.28 $cm^2.\mu m^{-1}.kg^{-1}$ (Table 4).

Before determining the morphological diffusion capacity of *I. iguana* lungs, we determined that 46.4 ± 4.3% of the diffusion barrier was composed of pulmonary epithelium, 32.4 ± 8.2% of capillary endothelium, and 21.2 ± 5.2% of connective tissue or basement membrane (Table 5). From these percentages and applying the respective Krogh diffusion constants (see Table 1), we calculated the morphological oxygen diffusion capacity in the lungs of *I. iguana* to vary between 1.6528 $ml.min^{-1}.kg^{-1}.mmHg^{-1}$ at 20 °C and 2.0504 $ml.min^{-1}.kg^{-1}.mmHg^{-1}$ at 37 °C (Table 6).

Table 5
Proportional distribution of pulmonary epithelium, capillary endothelium, and connective tissue/basal membrane within the diffusion barrier of the lungs of *Iguana iguana*. Sd: standard deviation.

Body mass (kg)	% pulmonary epithelium	% capillary endothelium	% connective tissue/ basal membrane
0.020	39.25	43.99	16.76
0.026	45.53	31.81	22.66
0.319	50.26	28.04	21.70
0.546	48.07	35.91	16.02
2.400	48.65	22.39	28.96
Mean	46.35	32.43	21.22
Sd	4.32	8.15	5.22

3.2. Comparative lung morphology

S_{AR} showed considerable variation in the analyzed species, being greatest in *V. exanthematicus* and smallest in *C. niloticus*. In relative terms and considering S_{AR} in *V. exanthematicus* being 100%, S_{AR} in *I. iguana* and *L. viridis* corresponded to 81% and 78%, respectively, S_{AR} in *S. merianae* was about half (54%), 38% in *T. scripta*, with *G. gecko* (17%)

Table 4
Stereological data from lungs of *Iguana iguana* (n = 5). Body mass (M_B); total lung volume (V_L); parenchymal volume (%P); parenchymal volume (V_P); total parenchymal surface area (S_A); respiratory surface area (%A_R); effective surface-to-volume ratio in parenchyma (S_{AR}/V_P); respiratory surface area (S_{AR}); harmonic mean thickness (τht); anatomical diffusion factor (ADF). Sd: standard deviation.

	M_B (kg)	V_L (ml. kg^{-1})	%P (% of V_L)	V_P (ml. kg^{-1})	S_A (10^3 cm^2. kg^{-1})	%A_R (% of S_A)	S_{AR}/V_P (cm^2. cm^{-3})	S_{AR} ($10^3 cm^2$. kg^{-1})	τht (μm)	ADF ($10^3.cm^2.\mu m^{-1}.kg^{-1}$)
1	0.020	335.00	11.94	40.20	0.11	68.80	139.34	5.57	0.76	7.26
2	0.026	330.80	13.95	49.60	0.09	40.62	79.33	3.66	0.65	5.61
3	0.319	284.30	18.19	52.00	1.05	35.68	63.98	3.30	0.58	5.64
4	0.546	238.50	19.89	47.50	2.78	59.69	107.71	5.10	0.66	7.74
5	2.400	199.20	25.52	50.80	10.51	58.72	86.22	4.38	0.51	8.50
Mean		277.56	17,89	48.02	2.90	52.70	95.31	4.40		6.95
Sd		58.83	5.32	4.67	4.38	13.96	29.20	0.95		1.28

Table 6
Morphological diffusion capacity for oxygen (DtO_2) in lungs of *Iguana iguana* at different temperatures. Sd: standard deviation.

	DtO_2 ($mlO_2.min^{-1}.kg^{-1}.mmHg^{-1}$)		
Body mass (kg)	20 °C	30 °C	37 °C
0.020	1.7282	1.9392	2.1440
0.026	1.3446	1.5087	1.6681
0.319	1.3437	1.5077	1.6670
0.546	1.8142	2.0357	2.2307
2.400	2.0332	2.2814	2.5223
Mean	1.6528	1.8546	2.0504
Sd	0.3068	0.3399	0.3732

and *C. niloticus* (12%) showing very small S_{AR} (Table 7). Species with unicameral lungs demonstrated a greater effective surface-volume ratio (S_{AR}/V_P) in the parenchyma than those with multicameral lungs, except for *G. gecko*. (Table 7).

The harmonic mean distance between the epithelial and endothelial surfaces gives the effective air-blood diffusion distance, varying in *I. iguana* between 0.51 and 0.76 μm. The other non-avian reptiles analyzed possesses diffusion distances between 0.5 and 1.40 μm. When comparing the seven species, we verified that the diffusion distances were independent of the type of lung being uni-, pauci-, or multicameral, with *G. gecko* (1.08 μm; unicameral lung) and *C. niloticus* (1.40 μm; multicameral lung) presenting the greatest diffusion distances.

Among non-avian reptiles, the calculated anatomical diffusion factor for *I. iguana* was 6.95 $cm^2.\mu m^{-1}.kg^{-1}$, similar to *S. merianae* (6.39), being somewhat smaller than the ADFs found in *V. exanthematicus* and *L. viridis*, but much greater than the ones found for *G. gecko* and *C. niloticus* (Table 4).

3.3. Principal component analysis

We selected the first three principal components (PC) of the PCA, corresponding to 80% of the total variance. PC1 (35.6%) was linked mainly to a smaller respiratory surface area (S_{AR} and S_A) and a lower diffusion capacity (ADF and τht), as well as to a lesser extent to lower lung volume (V_L; Fig. 2). This was reflected in physiological variables by a lower tidal volume (V_T), a slight drop in the rate of oxygen consumption, a small increase in respiratory frequency (f_R) and pulmonary ventilation ($\dot{V}_e$) (Table 8). This indicates that species having a small respiratory surface area (and partly low lung volumes) relative to their body size, compensate with a slight increase in breathing frequency. Positively linked to PC1 were: *Crocodylus niloticus* and *Gekko gecko*, while *Varanus exanthematicus* and *Iguana iguana* were inversely related to PC1. *Salvator merianae*, *Lacerta viridis*, and *Trachemys scripta* showed intermediate values (Fig. 2).

PC2 (26.7%) was mainly linked to a lower total parenchymal volume (V_P), with a low percentage of parenchyma concerning lung volume (%P), but with a great S_{AR}/V_P. To a lesser extent, it was linked to a lower V_L and a greater parenchymal surface area (S_A). From a physiological viewpoint, PC2 was linked to a considerable increase in f_R and increased $\dot{V}_e$. To a lesser extent, it was related to an increase in $\dot{V}O_2$ and a lower V_T (Table 8). Positively correlated to this axis were: *L. viridis, G. gecko, I. iguana*, and *S. merianae*, while *T. scripta*, *C. niloticus*, and *V. exanthematicus* were negatively related (Fig. 2).

PC3 (17.6%) was mainly linked to an increase in V_L and a reduction in the proportion of parenchyma concerning total volume (%P). To a lesser extent, it was related to a decrease in the ratio of the respiratory surface ($\%A_R$) and S_{AR}/V_P. PC3 was linked mainly to an increase in $\dot{V}O_2$ and V_T regarding physiological variables. To a lesser extent, it was related to a decrease in f_R (Table 8). This axis was positively associated with *I. iguana*, *G. gecko*, *V. exanthematicus*, and *C. niloticus*, while negatively related were *L. viridis*, *T. scripta*, and *S. merianae* (Fig. 2).

3.4. Phylogenetic analysis

The results from the phylogenetic signal analysis show that most morphological traits (%P, V_P, S_A, S_{AR}/V_P, S_{AR}, τht, and ADF) had a Blomberg's k value above 1 (see Table 9) — meaning that phylogenetically closer species tend to have morphological traits more similar than what would be expected under a Brownian Motion model. Although only S_{AR}/V_P had a significant p-value (<0.05), the other morphological traits also show a low probability for type I errors (all below 0.13), which suggests that the non-significance may be due to the small number of species analyzed. On the other hand, all physiological traits ($\dot{V}O_2$, V_T, f_R, and $\dot{V}_e$) had k values below 0.93 and all p-values above 0.4, indicating no phylogenetic signal in these traits. Altogether, these results imply that morphological traits tend to be phylogenetically more conserved than physiological traits (Figs. 3 and 4). The only exceptions were the morphological traits V_L and $\%A_R$, which, similar to the physiological traits, also presented k values below 1 with high p-values.

4. Discussion

Here, we described how the morphology of the respiratory system is related to physiological traits, further improving the understanding of the respiratory functions in non-avian reptiles— as well as other related functionalities, such as activity levels. The results of the phylogenetic signal tests also indicate that morphological traits are more likely to be evolutionary conserved along more comprehensive lineages than physiological traits, suggesting that evolutive physiological adaptations in the respiratory system could happen faster than morphological changes. Below we discuss the detailed interpretation of the results and their implications.

4.1. Morphological analysis

One difference of *Iguana iguana* lungs, when compared with the other non-avian reptiles in our study, is the fact that they possess lungs of the paucicameral type instead of unicameral (*Lacerta viridis, Salvator merianae, Gekko gecko*) or multicameral lungs (*Varanus exanthematicus*, *Crocodylus niloticus*, *Trachemys scripta*) (Perry et al., 1994). Non-avian reptiles (except crocodilians) have larger lungs than mammals and

Table 7
Relative differences in morphological variables. For variables total lung volume (V_L), parenchymal volume (%P), parenchymal volume (V_P), total parenchymal surface area (S_A), respiratory surface area ($\%A_R$), effective surface-to-volume ratio in parenchyma (S_{AR}/V_P), respiratory surface area (S_{AR}), harmonic mean thickness (τht), and anatomical diffusion factor (ADF) the greatest value was set to 100%, and for τht the smallest value was set to 100% and relative differences (in %) were calculated.

	V_L	%P	V_P	S_A	$\%A_R$	S_{AR}/V_P	S_{AR}	τht	ADF
Iguana iguana	91	40	41	47	60	66	81	137	83
Varanus exanthematicus	100	64	71	100	100	49	100	141	100
Lacerta viridis	31	77	27	99	79	97	78	115	96
Salvator merianae	28	58	19	61	88	100	54	100	77
Gekko gecko	54	26	16	23	78	27	17	235	11
Crocodylus niloticus	37	94	34	23	56	11	12	304	8
Trachemys scripta	86	100	100	41	93	13	38	109	50

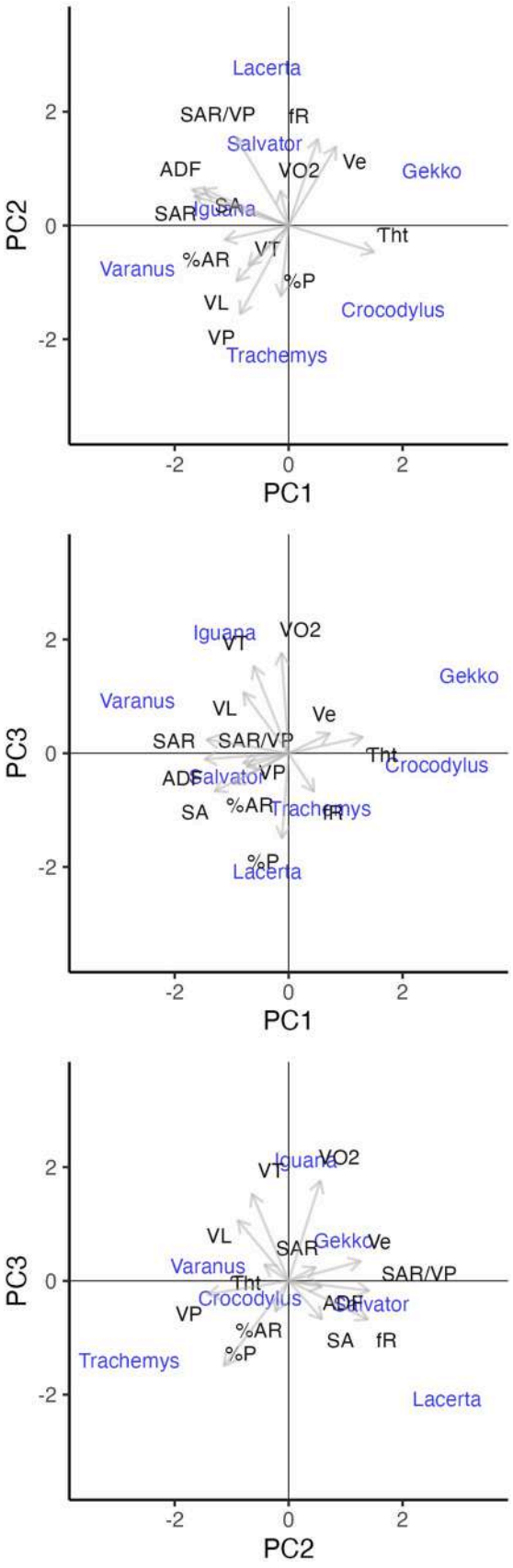

Fig. 2. Principal component analysis biplots depicting the relationship between morphological and physiological respiratory variables in non-avian reptile species.

birds (Perry, 1983; Souza et al., 2021) and *I. iguana* is no exception, only being surpassed in V_L by *V. exanthematicus*. Although there is significant variability among the non-avian reptiles analyzed, whether a lung is uni-, pauci-, or multicameral, the parenchyma may be more heterogeneously distributed in large lungs. The more sparsely partitioned regions of such lungs also show relatively poor vascularization or may even lack a pulmonary blood supply, as in some snakes. Therefore, lung volume is not necessarily related to lung diffusion capacity in non-avian reptiles. The large volume of heterogeneously partitioned lungs may serve several functions, some of which are not related to gas exchange (Duncker, 2004). For marine or aquatic species, the importance of the lungs as a buoyancy organ is evident (Perry, 1978). The large lung volume can also play a vital role in locomotion in many terrestrial lizards and snakes, ensuring optimal contact between the abdominal wall and the substrate. Another secondary function of large lungs may be important in species that consume large prey. The ventral and caudal lung portions, being in close contact with the esophagus and stomach, can generally be easily compressed without compromising the gas exchange conditions in the lung parenchyma during the ingestion and digestion of large prey items (Rosenberg, 1973).

The ultrastructure of *Iguana iguana* pulmonary epithelium does not differ from that reported for other non-avian reptiles (Peixoto et al., 2018). In this study, the parenchymal volume (%P) of *I. iguana* lungs showed to be smaller than in all the non-avian reptiles considered, except *G. gecko*, while V_P in *I. iguana* was between the one seen for the multicameral lungs (*T. scripta* and *V. examthematicus*), and the one seen in the unicameral lungs. This increase in V_P is expected (Peixoto et al., 2018) since greater pulmonary compartmentalization offers more surface area to carry respiratory parenchyma. In the case of *C. niloticus*, with its smaller lungs, parenchyma is distributed more homogeneously, meaning that the smaller V_L is more fully used than in larger lungs with a heterogeneous partition.

The anatomical diffusion factor (ADF) can be used to describe the overall morphological structure of lungs by combining respiratory surface area and air-blood diffusion distance. However, ADF values need to be evaluated with reservations despite showing similarities, since the same ADF can be obtained through different combinations of S_{AR} and τht (Perry, 1983). The ADF for the paucicameral iguana lung may be influenced by lung regions (cranial, medial and caudal) possessing different levels of gas exchange due to differences in vascularization, extension, and thickness of the respiratory parenchyma. Perry (1983) also comments that the ADF value represents only the anatomical hardware for gas exchange and indicates little about the respiratory surfaces' actual state of perfusion and ventilation. In *C. niloticus* with the lowest ADF of the analyzed species, blood flow to the lung varies with the ventilatory condition, increasing during breathing episodes and decreasing during non-ventilatory periods (Glass and Johansen, 1979). The same increase in perfusion is also observed in the lungs of *T. scripta*, contributing to the fast absorption of radioactive xenon gas in the parenchyma-rich, central lung region (Spragg et al., 1980).

Lambertz et al. (2015) hypothesized that the lungs of ancestral amniotes were multicameral, having been maintained in the lineages of synapsids, archosaurs, and testudines, while lung structure was simplified during a period of miniaturization of ancestral lepidosaurs, resulting in unicameral lungs predominating in extant species. Our morphological comparison revealed that lungs of varanids showed relatively greater values for several morphological traits. This possibly suggests that the secondary appearance of multicameral lungs in this lineage from a simpler uni- or paucicameral lung was not based on a *de novo* evolution of mutichamberedness, but maybe only reactivating the genetic program for multicameral lungs. Identifying the genetic markers for multicameral lungs and comparing them among amniotes should provide important insights into the pulmonary evolution of this taxon.

Table 8
Loads of variables in relation to the PCA axes. For description of variables see Tables 3 and 4. Color scale indicates the direction (blue negative, and red positive) and intensity (lighter colors are closer to zero) of variable correlation with the PCA axes.

	PC1	PC2	PC3
V_L	-0.2722077	-0.2417766	0.31697203
%P	0.04475251	-0.3763708	-0.4062719
V_P	-0.1842613	-0.4392669	-0.0666178
S_A	-0.3909738	0.18376505	0.05968109
$\%A_R$	-0.2095108	-0.1351866	-0.2526284
S_{AR}/V_P	-0.2336772	0.37578068	-0.2423866
S_{AR}	-0.4320328	0.10394792	-0.0640935
τht	0.37383984	-0.0808009	0.24349501
ADF	-0.42877	0.12488833	-0.1816309
$\dot{V}_{O_2}$	-0.1466842	0.22375462	0.46780442
V_T	-0.2317691	-0.1546597	0.47415889
f_R	0.14574168	0.38907774	-0.2247142
$\dot{V}_e$	0.17849831	0.39418183	0.11553363

Table 9
Phylogenetic signal results for each variable, with associated p-values.

	Blombergś k	p-value
V_L	0.86	0.586
%P	1.191	0.093
V_P	1.038	0.132
S_A	1.029	0.107
$\%A_R$	0.828	0.703
S_{AR}/V_P	1.391	0.01
S_{AR}	1.205	0.075
τht	1.135	0.091
ADF	1.245	0.061
$\dot{V}O_2$	0.821	0.685
V_T	0.807	0.718
f_R	0.807	0.757
$\dot{V}e$	0.935	0.404

4.2. Principal component analysis

To check the relationship between structure and function, we also analyzed the main components of the PCA *Iguana iguana*, *Lacerta viridis*, and *Salvator merianae* presented similar results when considering pulmonary morphology and physiology, with high PC2 and low PC1 values. This indicates that these species possess morphological and physiological characteristics to provide conditions for metabolic increases, such as seen in females during the reproductive period. Despite *Iguana iguana* having sedentary habits, the females can travel about 3 km from their riparian habitat towards beaches to nest and lay eggs (Morales-Mávil et al., 2007). In this process, with the production of eggs throughout the reproductive cycle, there is a significant increase in mass, which exerts a musculoskeletal demand for maintaining locomotor performance with

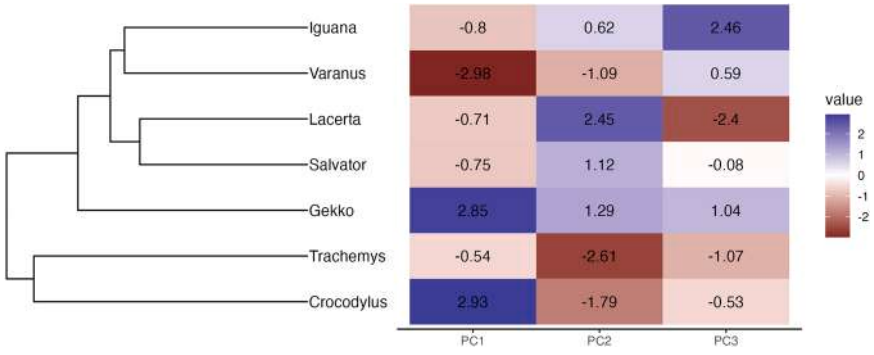

Fig. 3. Phylogenetic distribution of principal components summarizing the morphological and physiological respiratory variables in non-avian reptile species.

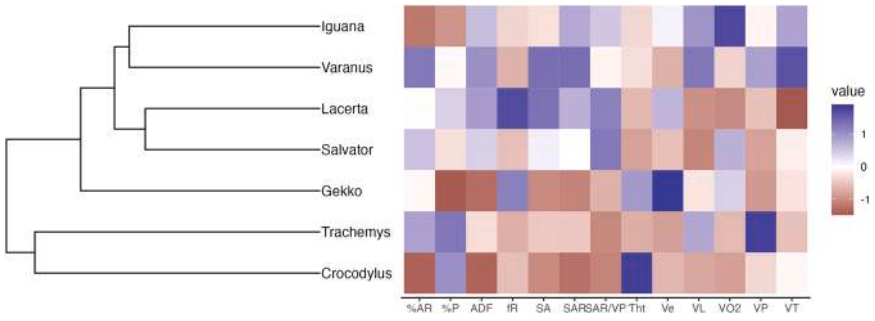

Fig. 4. Phylogenetic distribution of morphological and physiological respiratory variables in non-avian reptile species.

increased energy expenditure (Scales and Butler, 2007). In *Lacerta viridis* females active during the reproductive season, metabolic rates increase as demonstrated by higher rates of CO_2 production (Bradshaw et al., 1991). In *Salvator merianae*, the reproductive physiology of females supports the increase in metabolism associated with modulation of energy allocation during the annual cycles of folliculogenesis, nest building, and oviposition (Zena et al., 2019).

On the other hand, *Gekko gecko* appeared isolated with a high value of PC1 and PC2. This means that this species seems to have evolved a lung with a smaller respiratory surface and less diffusion capacity than the other analyzed Lepidosauria. Such pulmonary aspects of *G. gecko* seem to be associated with its sit-and-wait predatory habit, spending little time in locomotion (Aowphol et al., 2006). In this species, although breathing is arrhythmic and the respiratory rate is relatively low, breathing is a very explosive event, and the low rates result from prolonged periods of apnea.

Varanus exanthematicus showed low values for both PC1 and PC2, which indicates that this species has evolved to have a greater parenchymal volume, with a high percentage of parenchyma to lung volume and lower value of surface/volume ratio parenchyma, decreasing respiratory rate and total ventilation. Physiological results are also consistent with high aerobic capacities, with the voluntary activity of *V. exanthematicus* exceeding that of most other reptiles (Wood et al., 1978).

Crocodylus niloticus differs from the rest of the group with high PC1 and low PC2 values. This species, belonging to a lineage phylogenetically closer to the amniote ancestors, shows a reduced respiratory surface and a low diffusion capacity, with greater parenchymal volume, a high percentage of parenchyma to lung volume, but with a low surface/parenchymal volume ratio, decrease in respiratory rate (f_R) and consequently a lower rate of total ventilation. In the case of crocodilians, the group possesses a highly derived pulmonary ventilation system with the emergence of pelvic aspiration, involving the pelvic musculoskeletal system and the independently evolved diaphragmaticus muscles for accessory ventilatory functions (Farmer and Carrier, 2000). These authors also comment that it is difficult to reconcile these aspects with the low metabolic requirements and the sit-and-wait style of modern crocodilians. However, recent evidence suggests that endothermy evolved several times throughout the archosaurian radiation, including stem-pseudosuchia (Grigg et al., 2021), indicating the necessity for ventilatory specializations to sustain high aerobic activity and an ability to run and breathe simultaneously.

Trachemys scripta also showed a very low PC2 value. On the other hand, it differs from *C. niloticus* in that it shows intermediate values of PC1, i.e., intermediate values to the respiratory surface and oxygen diffusion capacity. This difference may be associated with different body plans, with *Trachemys* presenting a carapace that confers less compliance to the body wall. Instead of using intercostal muscles for ventilatory movements, they depend on muscles not associated with this function to move the entire visceral cavity to generate changes in lung volume and pressure (Souza and Klein, 2021).

Throughout this discussion, we observed that the morphological and physiological parameters of the analyzed non-avian reptile species were not always in a single direction, indicating possible different evolutionary paths to obtain O_2 in the face of specific demands in other environmental conditions.

4.3. Phylogenetic analysis

The results of the phylogenetic signal analysis indicated higher phylogenetic conservation in morphological traits compared to physiological traits. While preliminary (due to the small sample size), these findings suggest that respiratory physiological traits can evolve faster than the morphological traits in reptiles. A possible mechanism to explain such a result is provided by the cis-regulatory hypothesis, which suggests that the evolution of anatomic traits requires more genetic mutations than physiological traits because genes associated with physiological traits (physiogenes) are closer to terminal points of genetic regulatory networks, while genes linked to morphological changes (morphogenes) are located deeper in these networks (Carroll, 2005; Stern and Orgogozo, 2008). Moreover, previous studies have indicated that while morphogenes show higher rates of expression divergence, physiogenes have higher rates of protein sequence evolution and gains and loss of genes (Liao et al., 2010). Finally, morphogenes tended to be more essential than physiogenes — i.e, their loss may lead to infertility or death before puberty (Liao et al., 2010) — which, in turn, may lead to stronger adaptative regulation of these characteristics.

5. Conclusions

The integration between the morphological and physiological parameters of *I. iguana*, compared with other non-avian reptiles and the principal component analyzes, indicated relationships between morphology and physiology. Likewise, pulmonary morphometry showed a phylogenetic signal, suggesting being more conserved than physiological variables. In the sense of a possible morphological interrelation, we suggest that aspects of the respiratory morphology of the species in this study should not be interpreted only in terms of an exclusively respiratory function. Together, they can also work with other components of the body, such as muscles and skeleton, that provide the organism with an adequate supply of oxygen, ensuring energy for vital functions.

Therefore, future studies that evaluate the morphology of integrative organic systems may reveal new relationships with the physiology of non-avian reptiles and provide more comprehensive insights. Thus, supporting the notion that the integration of knowledge from different areas is necessary to understand the evolutionary history of vertebrate lineages.

Funding

WK was supported by a grant from the Conselho Nacional de

Desenvolvimento Científico e Tecnológico (CNPq; process n° 308249/2019–4).

CRediT authorship contribution statement

Conceptualization:A.L.C., W.K.; Methodology: A.L.C., B.V., WK; Formal analysis: A.L.C., B.V., WK.; Investigation: A.L.C., B.V., WK; Writing - original draft: A.L.C.; Writing - review & editing: A.L.C., B.V., WK; Project administration: AL.C., W.K.;Funding acquisition: W.K.

Declaration of Competing Interest

The authors declare that they have no conflict of interest.

Data Availability

Data will be made available on request.

Acknowledgments

ALC and WK dedicate this article to Prof. Dr. Steven Perry (Rheinische Friedrich-Wilhelms - Universität Bonn) for his inspirations regarding the evolution of respiratory systems. The authors thank Prof. Dr. Augusto Shinya Abe for the donation of the iguanas used and Barbara Champini for treating the grids used in Fig. 1.

References

Aowphol, A., Thirakhupt, K., Nabhitabhata, J., Voris, H.K., 2006. Foraging ecology of the Tokay gecko, *Gekko gecko* in a residential area in Thailand. Amphib. -Reptil 27, 491–503. https://doi.org/10.1163/156853806778877121.

Baker, L.A., White, F.N., 1970. Redistribution of cardiac output in response to heating in *Iguana iguana*. Comp. Biochem. Physiol. 35, 253–262.

Baker, L.A., Weathers, W.W., White, F.N., 1972. Temperature induced peripheral blood flow changes in lizards. J. Comp. Physiol. 80, 312–323.

Bartels, H., 1971. Diffusion coefficients and Krogh's diffusion constants: diffusion coefficients of gases in water. In: Altman, P.L., Dittmer, D.S. (Eds.), Respiration and Circulation. FASEB, Bethesda, MD, pp. 21–24.

Bradshaw, S.D., Saint Girons, H., Bradshaw, F.J., 1991. Seasonal changes in material and energy balance associated with reproduction in the green lizard, *Lacerta viridis*, in western France. In: Amphib-reptil, 12, pp. 21–32.

Brainerd, E.L., Moritz, S., Ritter, D.A., 2016. XROMM analysis of rib kinematics during lung ventilation in the green iguana, *Iguana iguana*. J. Exp. Biol. 219, 404–411. https://doi.org/10.1242/jeb.127928.

Brown, C.R., Loveridge, J.P., 1981. The effect of temperature on oxygen consumption and evaporative water loss in *Crocodylus niloticus*. Comp. Biochem. Physiol. A 69, 51–55.

Carrier, D.R., 1987. Lung ventilation during walking and running in four species of lizards. Exp. Biol. 47, 33–42.

Carroll, S.B., 2005. Evolution at two levels: on genes and form. Plos Biol. 3, 1159–1166. https://doi.org/10.1371/journal.pbio.0030245.

Chiu, K.W., Sham, J.S.K., Maderson, P.F.A., Zucker, A.H., 1986. Interaction between thermal environments and hormones affecting skin-shedding frequency in the tokay (*Gekko gecko*) (Gekkonidae, Lacertilia). Comp. Biochem. Physiol. A 84, 345–351.

Cieri, R.L., Craven, B.A., Schachner, E.R., Farmer, C.G., 2014. New insight into the evolution of the vertebrate respiratory system and the discovery of unidirectional airflow in iguana lungs. PNAS 111, 17218–17223. https://doi.org/10.1073/pnas.1405088111.

Cragg, P., 1978. Oxygen consumption in the lizard genus *Lacerta* in relation to diel variation, maximum activity and body weight. J. Exp. Biol. 77, 33–56. https://doi.org/10.1242/Jeb.77.1.33.

Duncker, H.-R., 2004. Vertebrate lungs: structure, topography and mechanics. A comparative perspective of the progressive integration of respiratory system, locomotor apparatus and ontogenetic development. Respir. Physiol. Neurobiol. 144, 111–124. https://doi.org/10.1016/j.resp.2004.07.020.

Farmer, C.G., Hicks, J.W., 2000. Circulatory impairment induced by exercise in the lizard *Iguana iguana*. J. Exp. Biol. 203, 2691–2697. https://doi.org/10.1242/jeb.203.17.2691.

Giordano, R.V., Jackson, D.C., 1973. The effect of temperature on ventilation in the green iguana (*Iguana iguana*). Comp. Biochem. Physiol. A 45, 235–238.

Glass, M.L., Johansen, K., 1979. Periodic breathing in the crocodile, *Crocodylus niloticus*: consequences for the gas exchange ratio and control of breathing. J. Exp. Zool. 208, 319–326.

Gleeson, T.T., Mitchell, G.S., Bennett, A.F., 1980. Cardiovascular responses to graded activity in the lizards *Varanus* and *Iguana*. Am. J. Physiol. 239, R174–R179.

Grigg, G., Nowack, J., Bicudo, J.E.P.W., Bal, N.C., Woodward, H.N., Seymour, R.S., 2021. Whole-body endothermy: ancient, homologous and widespread among the ancestors of mammals, birds and crocodylians. Biol. Rev. 97, 766–801.

Grote, J., 1967. Die Sauerstoffdiffusionskonstanten im Lungengewebe und Wasser und ihre Temperaturabhängigkeit. Pflüg. 'S. Arch. für die Gesamt Physiol. Des. Mensch und der Tiere 295, 245–254.

Hicks, J.W., Wang, T., Bennett, A.F., 2000. Patterns of cardiovascular and ventilatory response to elevated metabolic states in the lizard *Varanus exanthematicus*. J. Exp. Biol. 203, 2437–2445. https://doi.org/10.1242/jeb.203.16.2437.

Howard, C.V., Reed, M.G., 2005. Unbiased stereology: three-dimensional measurement in microscopy, 2th ed. Garland Science/BIOS Scientific Publishers, New York.

Jackson, D.C., 1971. The effect of temperature on ventilation in the turtle *Pseudemys scripta elegans*. Respir. Physiol. 12, 131–140.

Klein, W., Andrade, D.V., Abe, A.S., Perry, S.F., 2003. Role of the post-hepatic septum on breathing during locomotion in Tupinambis merianae (Reptilia: Teiidae). J. Exp. Biol. 206, 2135–2143. https://doi.org/10.1242/jeb.00400.

Krogh, A., 1919. The supply of oxygen to the tissues and the regulation of the capillary circulation. J. Physiol. 52, 457–474.

Kumar, S.M., Suleski, J.E., Craig, A.E., Kasprowicz, M., Sanderford, M., Li, M., Stecher, G., Hedges, S.B., 2022. TimeTree 5: An expanded resource for species divergence times. Mol. Biol. Evol. https://doi.org/10.1093/molbev/msac174.

Lambertz, M., Grommes, K., Kohlsdorf, T., Perry, S.F., 2015. Lungs of the first amniotes: why simple if they can be complex? Biol. Lett. 11, 20140848 https://doi.org/10.1098/rsbl.2014.0848.

Liao, B.Y., Weng, M.P., Zhang, J., 2010. Contrasting genetic paths to morphological and physiological evolution. PNAS 107, 7353–7358. https://doi.org/10.1073/pnas.091033910.

Maxwell, L.K., Jacobson, E.R., McNab, B.K., 2003. Intraspecific allometry of standard metabolic rate in green iguanas, *Iguana iguana*. Comp. Biochem. Physiol. 136, 301–310. https://doi.org/10.1016/s1095-6433(03)00145-4.

Mitchell, G.S., Gleeson, T.T., Bennett, A.F., 1981. Pulmonary oxygen transport during activity in lizards. Respir. Physiol. 43, 365–375.

Moraes, M.F.P.G., Höller, S., da Costa, O.T.F., Glass, M.L., Fernandes, M.N., Perry, S.F., 2005. Morphometric comparison of the respiratory organs in the South American lungfish *Lepidosiren paradoxa* (Dipnoi). Physiol. Biochem. Zool. 78, 546–559. https://doi.org/10.1086/430686.

Morales-Mávil, J.E., Vogt, R.C., Gadsden-Esparza, H., 2007. Desplazamientos de la iguana verde, *Iguana iguana* (Squamata: Iguanidae) durante la estación seca en La Palma. Rev. Biol. Trop. 55, 709–715.

Peixoto, D., Klein, W., Abe, A.S., Cruz, A.L., 2018. Functional morphology of the lungs of the green iguana, *Iguana iguana*, in relation of body mass (Squamata: Reptilia). Vert. Zool. 68, 64–82.

Perry, S.F., 1978. Quantitative anatomy of the lungs of the red eared turtle, *Pseudemys scripta elegans*. Resp. Physiol. 35, 245–262.

Perry, S.F., 1983. Reptilian lungs: functional anatomy and evolution. Adv. Anat. Embryol. Cell Biol. 79, 1–81.

Perry, S.F., Hein, J., Vandieken, E., 1994. Gas-exchange morphometry of the lungs of the Tokay, *Gekko gecko* L (Reptilia, Squamata, Gekkonidae). J. Comp. Physiol. B 164, 206–214. https://doi.org/10.1007/BF00354081.

Perry, S.F., 1998. Lungs: comparative anatomy, functional morphology, and evolution. In: Gans, C., Gaunt, A.S. (Eds.), Biology of the Reptilia, Vol. 19. Society for the Study of Amphibians and Reptiles, Ithaca, New York, pp. 1–92.

Perry, S.F., Lambertz, M., Schmitz, A., 2019. Respiratory Biology of Animals: Evolutionary And Functional Morphology. Oxford University Press, New York.

Perry, S.F., Sander, M., 2004. Reconstructing the evolution of the respiratory apparatus in tetrapods. Respir. Physiol. Neurobiol. 144, 125–139. https://doi.org/10.1016/j.resp.2004.06.018.

R Core Team, 2021. R: A Language and Environment for Statistical Computing. R Foundation for Statistical Computing, Vienna, Austria (URL). https://www.R-project.org/.

Revell, L.J., 2012. phytools: An R package for phylogenetic comparative biology (and other things). Methods Ecol. Evol. 3, *217*–223. https://doi.org/10.1111/j.2041-210X.2011.00169.x.

Rosenberg, H.I., 1973. Functional anatomy of pulmonary ventilation in the garter snake, *Thamnophis elegans*. J. Morphol. 140, 171–184. https://doi.org/10.1002/(ISSN)1097-4687.

Sartori, M.R., Abe, A.S., Crossley II, D.A., Taylor, E.W., 2017. Rates of oxygen uptake increase independently of changes in heart rate in late stages of development and at hatching in the green iguana, *Iguana iguana*. Comp. Biochem. Physiol. A 205, 28–34. https://doi.org/10.1016/j.cbpa.2016.12.020.

Scales, J., Butler, M., 2007. Are powerful females powerful enough? Acceleration in gravid green iguanas (*Iguana iguana*). Integr. Comp. Biol. 47, 285–294. https://doi.org/10.1093/icb/icm054.

Souza, R.B.B., Bonfim, V.M.G., Rios, V.P., Klein, W., 2021. Allometric relations of respiratory variables in Amniota: effects of phylogeny, form, and function. Comp. Biochem. Physiol. A 252, 110845. https://doi.org/10.1016/j.cbpa.2020.110845.

Souza, R.B.B.d., Klein, W., 2021. The influence of the post-pulmonary septum and submersion on the pulmonary mechanics of Trachemys scripta (Cryptodira: Emydidae). J. Exp. Biol. 224 https://doi.org/10.1242/jeb.242386.

Spragg, R.G., Ackerman, R., White, F.N., 1980. Distribution of ventilation in the turtle *Pseudemys scripta*. Respir. Physiol. 42, 73–86.

Stern, D.L., Orgogozo, V., 2008. The loci of evolution: How predictable is genetic evolution? Evolution 62, 2155–2177. https://doi.org/10.1111/j.1558-5646.2008.00450.x.

Tucker, V.A., 1968. Oxygen transport by the circulatory system of the Green Iguana (*Iguana iguana*) at different body temperatures. J. Exp. Biol. 44, 77–92.

Wang, T., Carrier, D.R., Hicks, J.W., 1997. Ventilation and gas exchange in lizards during treadmill exercise. J. Exp. Biol. 200, 2629–2639. https://doi.org/10.1242/jeb.200.20.2629.

Wang, T., Smits, A.W., Burggren, W.W., 1998. Pulmonary function in reptiles. In: Gans, C., Gaunt, A.S. (Eds.), Biology of the Reptilia, Vol. 19. Society for the Study of Amphibians and Reptiles, Ithaca, New York, pp. 297–374.

Wang, T., Hicks, J.W., 2002. An integrative model to predict maximum O_2 uptake in animals with central vascular shunts. Zoology 105, 45–53. https://doi.org/10.1078/0944-2006-00043.

Wood, S.C., Moberly, W.R., 1970. The influence of temperature on the respiratory properties of iguana blood. Respir. Physiol. 10, 20–29.

Wood, S.C., Johansen, K., Glass, M.L., Maloiy, G.M.O., 1978. Aerobic metabolism of the lizard *Varanus exanthematicus:* effects of activity, temperature, and size. J. Comp. Physiol. B 127, 331–336.

Zena, L.A., Dillon, D., Hunt, K.E., Navas, C.A., Bícego, K.C., Buck, C.L., 2019. Seasonal changes in plasma concentrations of the thyroid, glucocorticoid and reproductive hormones in the tegu lizard *Salvator merianae*. Gen. Comp. Endocrinol. 273, 134–143. https://doi.org/10.1016/j.ygcen.2018.06.006.